IMPROVEMENT OF BEAM IMAGING SYSTEMS THROUGH OPTICS PROPAGATION SIMULATIONS*

B. Bolzon[#1,2,3], T. Lefevre[1], S. Mazzoni[1], C. P. Welsch[2,3], P. Karataev[4], K. Kruchinin[4], A. Aryshev[5]
[1] CERN, Geneva, Switzerland
[2] Cockcroft Institute, Warrington, Cheshire, U.K.
[3] The University of Liverpool, Liverpool, U.K.
[4] J.A.I. at Royal Holloway, University of London, Egham, Surrey, U.K.
[5] KEK, Tsukuba, Ibaraki, Japan

Abstract

Optical Transition Radiation (OTR) is emitted when a charged particle crosses the interface between two media with different dielectric properties. It has become a widespread method for beam profile measurements. However, there are no tools to simulate the propagation of the OTR electric field through an optical system. Simulations using ZEMAX have been performed in order to quantify optical errors, such as aberrations, diffraction, depth of field and misalignment. This paper focuses on simulations of vertically polarized OTR photons with the aim of understanding what limits the resolution of realistic beam imaging systems.

INTRODUCTION

In accelerators, OTR beam imaging systems are widely used to determine the properties of a particle beam. The OTR photons are typically transported through a number of optical elements, such as lenses, filters, mirrors up to a camera. The Point Spread Function (PSF), which is defined in this case as the image of the radiation field generated by a single particle, represents the resolution of the particle beam imaging system. It depends thus on the source field distribution, the radiation wavelength and the imperfections of the optical system.

The PSF of beam imaging systems has been extensively studied for sub-micrometre resolution [1-3]. Analytical calculations were used to propagate the electric field using diffraction laws through ideal lenses (thin lens approximation). Optical errors, such as aberrations, could not be predicted accurately enough and the resolution of OTR system was limited experimentally to few micrometres.

In order to understand these limitations and to improve the resolution of such systems, numerical simulations have been performed using the Physical Optics Propagation mode (POP) of ZEMAX, which uses diffraction laws to propagate the OTR field through realistic optical components [4]. The latter offers a large database of commercially available optical components (lenses, viewports, polarizers…), which can be used to simulate any optical system and evaluate the different errors occurring along the optical line.

This paper presents simulations of the propagation of the OTR electric field in both near and far field conditions. Simulations of the OTR PSF are shown for different energies, optical wavelengths and lenses, and the impact of offset of optical elements on the PSF is analysed. Simulations are also compared to experimental data, obtained on the ATF2 facility at KEK. Finally, the resolution and the accuracy of the OTR beam imaging systems are discussed.

FREE SPACE PROPAGATION

Assuming free space propagation and relativistic beam energies, far field conditions would apply at a distance from the source $L >> \lambda*\gamma$, with λ the radiation wavelength, γ the charged particle Lorentz factor [5] [6]. Hence, in accelerators, near field conditions must be considered in most cases since optical elements are generally located at rather short distances from the source.

Figure 1 shows the OTR angular distribution calculated by ZEMAX for a wavelength of 550 nm and for different energies. In far field (up to γ~500), the first maximum is at $1/\gamma$ [7] and the peak intensity is proportional to γ^2. In near field, the angular distribution does not depend anymore on γ [8]. A perfect matching between ZEMAX simulations and analytical calculations for optical transition and diffraction radiation is shown here [9].

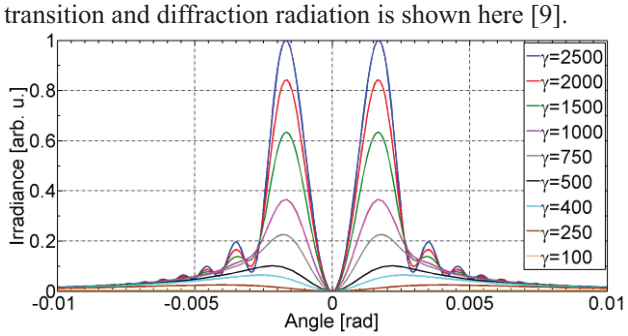

Figure 1: OTR angular distribution calculated by ZEMAX for λ=550 nm and for different energies.

The OTR spatial distribution at the source extends radially as $\lambda*\gamma$. While the required computing time and resources increase, the simulation of all the OTR tails is essential. If not, an artificial diffraction effect would occur at the source and the angular distribution would be seen wider than it should be. Tails have also a large impact on diffraction when going through narrow apertures such as lenses [1]. The PSF may thus not be simulated accurately.

#Benoit.Bolzon@cern.ch

ISBN 978-3-95450-132-8

OTR PSF

Recommendations about Resolution

At the Accelerator Test Facility 2 (ATF2), a monitor installed at the beginning of the Final Focus System enabled the first observation of the OTR PSF with few micrometres of resolution [10]. At ATF2, the electron beam energy corresponds to γ of 2,500.

An improvement of the optical system was studied with ZEMAX using achromat doublet lens DLB-30-120-PM from Sigma-Koki. The system magnification was 7.39. This upgrade was implemented in 2013 to allow measurements with sub-micrometre resolution [11] in good accordance with ZEMAX predictions.

The OTR PSF has been simulated for λ=550 nm and for different energies, as depicted in Fig. 2. It varies very little with energy, from a distance between peaks of 6.0 μm for γ =50 to 7.1 μm for γ=2,500. In fact, the source size is much smaller than the lens diameter [3] (source diameter of 2*λ*γ=2.75 mm at γ=2,500 and λ=550 nm to be compared to a lens diameter of 30 mm).

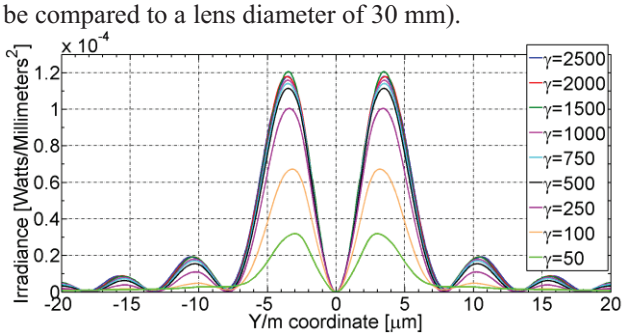

Figure 2: OTR PSF distribution calculated by ZEMAX for λ=550 nm and for different energies.

In Fig. 3, the OTR PSF has been simulated for different wavelengths (with a focus adjusted accordingly for each wavelength). Diffraction at the source is smaller for shorter wavelength, and the PSF is reduced accordingly. Based on this fact, using ultra-violet (UV) optics may then provide even smaller PSF and better resolution.

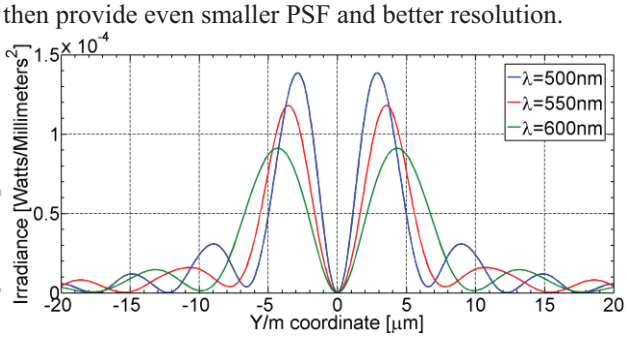

Figure 3: OTR PSF distribution calculated by ZEMAX for γ=2,500 and for 500, 550 and 600 nm wavelengths.

Figure 4 represents the OTR PSF at the paraxial focus (magnification of 7.39) for 3 lenses of 30 mm diameter and 100 mm focal length: A plano-convex lens (SLB-30-100-PY2 from Sigma-Koki) and an achromat doublet lens (DLB-30-100-PM from Sigma-Koki) both optimized for visible light (400 nm) and a third lens optimized for the UV light (achromat doublet lens 027-3020 from OptoSigma). The achromat lens gives a smaller PSF than the plano-convex lens since chromatic and geometric aberrations are better corrected. It also provides a smaller PSF than the UV achromat lens. Even if using shorter wavelength was expected to reduce diffraction effects, UV materials induce larger aberrations, which clearly limit the use of such lenses. An alternative solution may be to work in the UV domain with reflective optics (such as elliptical mirrors).

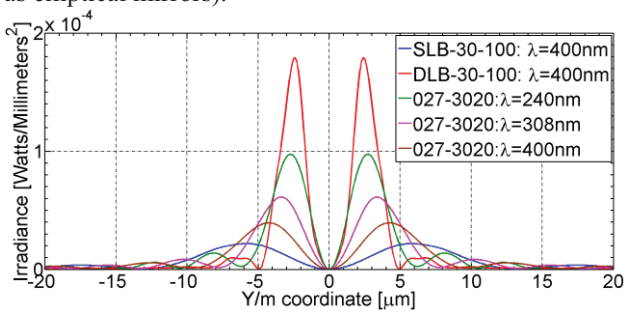

Figure 4: OTR PSF distribution calculated by ZEMAX for different types of lenses and for γ of 2,500.

ZEMAX offers the possibility to study in detail the evolution of the PSF with respect to optical imperfection. For example, the PSF has been simulated for different vertical offsets of the achromat doublet lens. The results are presented in Fig. 5. Even if the FWHM of the PSF does not change significantly for an offset of ±2 mm (from 10.7 μm to 12.2 μm), the visibility I_{min}/I_{max} (I_{min}: minimum value of the intensity between the two lobes; I_{max}: peak intensity of the highest lobe) is strongly modified. This has a large impact on the accuracy of the beam size measurement extracted from the PSF visibility as seen later. Such offsets introduce also an asymmetry of the distribution, which would suggest that a better alignment of the lens should be performed.

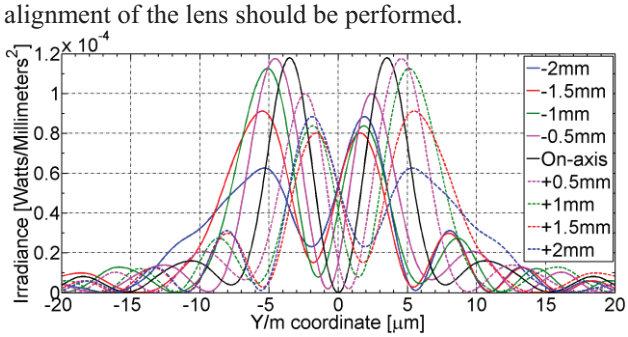

Figure 5: OTR PSF distribution calculated by ZEMAX for different lens offsets (λ=550 nm; γ=2,500).

Minimum Resolution Using Visible Light

Diffraction effects and aberrations have been studied both theoretically and experimentally. For that purpose, a motorized iris has been inserted in front of the achromat lens of the ATF2 optical system. The measured and simulated distance between peaks and FWHM of the PSF are shown as a function of the iris diameter in Fig. 6. The size of the PSF increases as the diameter of the iris gets smaller. The optical system is thus diffraction limited for

iris diameters smaller than 18mm. A theoretical diffraction curve has been added on Fig. 6 for comparison. For iris diameters larger than 18 mm, the experimental data are higher than the theoretical diffraction curve, which would indicate that the system is dominated by aberrations. The minimum distance between peaks obtained experimentally was of 6.4 μm and the smallest measured beam size was 1.7 μm FWHM [12]. This corresponded to a visibility of the PSF of 0.13.

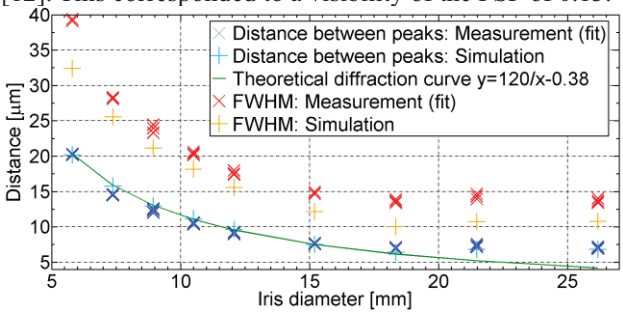

Figure 6: OTR PSF size (distance between peaks and FWHM) for different iris diameters (λ=550 nm; γ=50).

BEAM SIZE EXTRACTION FROM PSF

On ATF2, the horizontal beam size is large compared to the PSF. It is extracted by fitting the horizontal beam profile obtained from the image with a Gaussian distribution with a given σ or FWHM. The vertical beam size is smaller or equal to the PSF and it is extracted from the visibility of the PSF [12] [13].

Figure 7 presents the expected PSF distributions at ATF2 (ATF2 PSF FWHM=9.9 μm) assuming Gaussian beam distribution with sigmas ranging from 20 μm down to 100 nm. Simulations were performed with the achromat doublet lens DLB-30-120-PM.

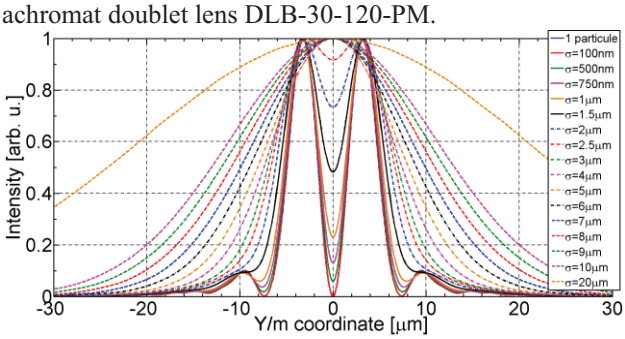

Figure 7: Convolution of ATF2 OTR PSF with a Gaussian distribution for different beam sizes (λ=550 nm; γ=50).

The corresponding measured FWHM beam sizes are reported on Fig. 8 as well as the errors made on the measurements. The PSF visibility method can be applied for beam sizes ranging from 1.7 μm up to 6 μm FWHM with visibilities of 0.13 and 0.92 respectively.

For slightly larger beam sizes the visibility of the two lobes disappears and the errors made of the FWHM of the distribution is significant. A maximum error of 98% is made for an input beam size of 7 μm FWHM. As the beam size increases, the error diminishes. For a FWHM of 45 μm the error reduces to 3%.

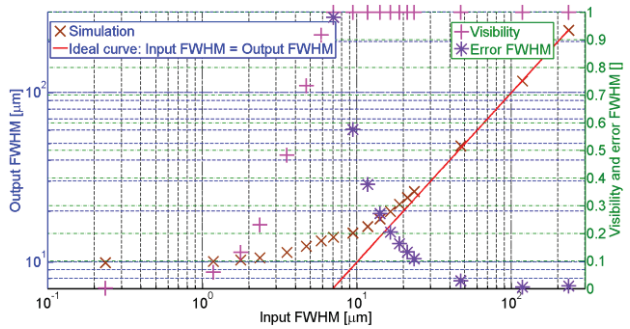

Figure 8: Measured beam size versus real beam size

With horizontal beam sizes on ATF2 around 150 μm sigma, the error made on this measurement is negligible.

CONCLUSION

ZEMAX allows very accurate simulations to predict the performance of any Optical Transition Radiation imaging system. The OTR Point Spread Function can be obtained taking into account realistic optical components and their limitations.

An optimization of the ATF2 high-resolution OTR system allowed performing vertical beam size measurements below 1 μm sigma.

The misalignment of optical components, such as lenses, has been studied and showed an asymmetry of the PSF and a reduction of its visibility, leading to a degradation of the resolution of the imaging system.

For beams with transverse size similar or slightly larger than the PSF, our simulations indicated that the measured beam profile would differ from what it should be. Errors can be as large as a factor 2. These systematic errors should be taken into account in the data analysis. This clearly underlines the importance of having a powerful tool for simulating in detail OTR imaging systems.

Our future study will investigate the possibility to design an imaging system working in the UV regime with a telescope made out of elliptical mirrors. This particular arrangement is expected to reduce diffraction, to minimize aberrations and to provide a high magnification as required for high-resolution profile measurements.

REFERENCES

[1] M. Castellano et al., Phys Rev STAB 1, 062801 (1998).
[2] A.P. Potylitsyn, Adv. Rad. Sources and App., Vol., 199, (2006) 149-163.
[3] P. Karataev, Phys. Let A 345 (2005) 428-438.
[4] Zemax user's manual, 8th October, 2013.
[5] V.A. Verzilov, Phys. Lett. A 273 (2000) 135.
[6] R.A. Bosch, Nucl. Instr. and Meth. A 431 (1999) 320.
[7] E. Bravin, T. Lefevre, Proc. DIPAC, PM03, Mainz (2003).
[8] G. Kube, March 18, TESLA-FEL 2008-01, equation 29.
[9] T. Aumeyr et al., Journal of Physics: Conference Series 517 (2014) 012026.

ISBN 978-3-95450-132-8

[10] P. Karataev et al., PRL 107, 174801 (2011).
[11] B. Bolzon et al., Proc. IBIC2013, MOPF04, http://jacow.org/.
[12] K. Kruchinin et al., Proc. IBIC2013, WEAL2, http://jacow.org/.
[13] K. Kruchinin et al., Journal of Physics: Conference Series 517 (2014) 012011

ISBN 978-3-95450-132-8